

Influence of atmospheric turbulence on the accuracy of lidar measurements of aerosol concentration integral parameters in plumes

V.P. Kabashnikov and A.P. Chaykovskii

*B.I. Stepanov Institute of Physics,
National Academy of Sciences of Belarus, Minsk*

Received June 7, 2006

A technique for lidar sensing of aerosol plumes aiming at estimation of the point stationary source capacity is considered. Influence of atmospheric turbulence on the accuracy of lidar measurements of aerosol concentration integral parameters is studied. The measurement error is shown to be determined by the first- and second-order statistical moments of the contaminant concentration integral along the sensing path. The error depends on turbulence parameters, distance between the sensing flow part and the contaminant source, as well as instants of pulsing and coordinates of sensing beams.

Introduction

The development of laser sensing techniques and lidar equipment expand the range of lidar application in the systems of air monitoring in industrial regions. The use of lidars is necessary, when on-line remote data on 3D distribution of contaminants are required. The practical tasks, where lidars are used, are the monitoring of aerosol concentration distribution in industrial plumes and estimate of the emission intensity.^{1–6}

The idea of measuring the capacity of a stationary contaminant source consists in measuring the concentration integral over an arbitrary plume cross section and its consequent multiplying by the wind velocity.^{1–3,7} The result is the contaminant flow magnitude, which in stationary case is equal to the emission source capacity.

Although the idea itself is simple, a number of methodical questions should be solved and the obtained reliability estimated before its practical realization. Of interest in this case is the problem of determining the contaminant concentration from the measured lidar signal. To do this, the coefficient of attenuation or backscattering along the sensing path is first determined from the measured lidar signal.

Possible significant optical depths of aerosol flows and uncertainty of some optical parameters of aerosol particles can introduce some difficulties, first of all, the lidar ratio, i.e., the ratio of the attenuation coefficient to the backscattering one. The contamination concentration is calculated based on the correlation between optical and microphysical parameters of aerosol particles.

The main uncertainty factor at this stage is variability of the contaminant composition and microstructure. In general, the success of lidar technique essentially depends on additional optical and other measurements of parameters of

contaminants and the atmosphere, which allow meaningful estimate of the parameters used in algorithms of the lidar data processing.

The listed-above questions are of principle importance for many applications of the lidar sensing technique requiring a detailed methodical elaboration.^{1–6} Another part of the problem, still insufficiently studied, concerns the turbulent character of the wind velocity field and contaminant concentration fluctuations in the plume. Finally, turbulent fluctuations of contaminant concentrations in the plume introduce an additional uncertainty in determining the source emission capacity. The equation for one-point temporal correlation function for fluctuations of the reflected optical radiation due to atmospheric turbulence was obtained in Ref. 8. However, the specific character of lidar measurements of aerosol emission intensity requires the knowledge of spatiotemporal correlation functions.

In this work, the significance of atmospheric turbulence for measurements of the lidar emission intensity at arbitrary distances from the source is estimated on the base of the plume model considering intra-plume concentration fluctuations.

Technique for lidar sensing of contaminant flows

Introduce the Cartesian coordinate system, where x axis is directed along the mean wind direction and z axis is directed upward. Take that an aerosol flow is sensed from one side in a vertical plane normal to the mean wind direction (Fig. 1).

Sensing angle intervals are chosen larger than the angular size of the region of probable plume location. It is supposed that the lidar is located at the distance much larger than the plume cross section size, therefore the non-parallelism of “crossing” parts

of sensing paths within the plume zone are negligible. The fractional error in determination of concentration integral over cross section due to the non-parallelism equals to the plume angular size.

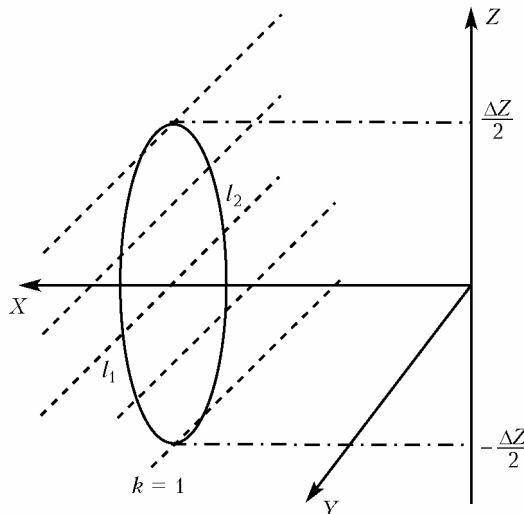


Fig. 1. Geometry of the experiment.

Flow rate in the plume becomes virtually equal to the wind velocity at some distance from the chimney's orifice. This distance depends on the ratio of initial outflow velocity to wind velocity, levels of overheating, and atmospheric stratification. The distance can be estimated based on the calculations of the structure of heated streams in a carrying away flow.⁹ If the ratio of the initial outflow velocity to the wind velocity is equal to 5 or 2.5, then the above distance is within 20–40 radii of the chimney orifice at a neutral and stable stratification, 60–80 radii at neutral, and more than 100 radii at unstable atmospheric stratification.⁹ Neglecting the diffusion along the plume axis in comparison with wind transfer and considering the influence of atmospheric aerosol on the particle concentration in the plume as negligibly small, the capacity M of a stationary source can be approximately presented as the integral of the turbulence-averaged concentration over the arbitrary plume cross section multiplied by the average wind velocity U :

$$M = U \bar{\eta}(x, z) dz, \quad (1)$$

where η is the linear integral of the contaminant concentration along the sensing path part crossing the plume; the bar designates the turbulence averaging. The average wind velocity can be determined from data of ground weather stations and known model relations between wind velocities near surface and at a height.¹⁰ The data on direct lidar or sodar velocity measurements at a height can be used.

The integral η is defined from the plume optical depth or from the integral value of the backscattering coefficient, retrieved from the lidar data. Optical

contaminant parameters are obtained from the solution of the lidar equation

$$S(l) = A(\beta_a(l) + \beta_m(l)) \exp[-2(\tau_a(l) + \tau_m(l))], \quad (2)$$

where A is the instrument parameter, which can be considered as constant beyond the nearest zone; $S(l) = P(l)l^2/W_0$ is the corrected lidar signal; $P(l)$ is the lidar signal; l is the distance along the sensing path; W_0 is the energy of the sensing pulse; $\tau_a = \int_0^l \sigma_a dl$ and $\tau_m = \int_0^l \sigma_m dl$ are the aerosol and molecular optical depths; σ_a and σ_m are the coefficients of aerosol and molecular attenuation; β_a and β_m are the coefficients of aerosol and molecular backscattering.

When solving lidar equation (2), the additional parameters are introduced: the aerosol ($\gamma_a(l) = \sigma_a/\beta_a$) depending on aerosol particle microstructure and molecular ($\gamma_m = \sigma_m/\beta_m = \text{const}$) lidar ratios. To estimate the emission source capacity, the distribution of optical parameters along the sensing path needs not to be recovered. It is sufficient to determine the optical depth at the sensing path's segment (l_1, l_2) crossing the plume. The required solution can be obtained by putting Eq. (2) in the form

$$q(l) = A\tau'_{\text{eff}} \exp[-2\tau_{\text{eff}}], \quad (3)$$

where

$$q(l) = S(l)\gamma_a \exp\left[-2 \int (\gamma_a/\gamma_m - 1)\sigma_m dl\right]; \quad (4)$$

$$\tau_{\text{eff}} = \int_0^l (\sigma_a + \sigma_m \gamma_a/\gamma_m) dl, \quad (5)$$

$\tau'_{\text{eff}} = \sigma_a + \sigma_m \gamma_a/\gamma_m$ is the coordinate derivative of τ_{eff} along the sensing path.

Integrating both parts of Eq. (4) over the segment (l_1, l_2), we obtain

$$Q(l_2, l_1) = \int_{l_1}^{l_2} q(l) dl = -0.5A[\exp(-2\tau_{\text{eff}}(l_2)) - \exp(-2\tau_{\text{eff}}(l_1))]. \quad (6)$$

As it follows from Eq. (6),

$$\tau_a(l_2, l_1) = -0.5 \ln(1 - 2Q(l_2, l_1)/AT^2(l_1)) - \int_{l_1}^{l_2} \sigma_m \gamma_a/\gamma_m dl. \quad (7)$$

Here $T(l_1) = \exp(-\tau_a(l_1) + \tau_m(l_1))$ is the optical depth of the sensing path's segment up to a flow; the parameter

$$Q(l_2, l_1) = \int_{l_1}^{l_2} S(l)\gamma_a \exp\left[-2 \int_{l_1}^l (\gamma_a/\gamma_m - 1)\sigma_m dl\right] dl \quad (8)$$

is the accumulated signal $S(l)$ with the weight function

$$\gamma_a \exp\left(-2 \int (\gamma_a/\gamma_m - 1) \sigma_m dl\right)$$

at the segment (l_1, l_2) . Equation (7) is the lidar equation solution by the "integral accumulation" method.¹ Differentiating Eq. (7), the known Fernald–Klett solutions for σ_a and β_a can be obtained. When processing real experimental data, γ_a is usually considered constant, because data on its spatial variability are lacking.

An essential problem for the considered task is the lidar calibration, i.e., determination of A . The choice of calibration technique is usually determined by the presence of equipment for independent measurements of optical atmospheric parameters. When sensing aerosol vertically, the measurement data in high atmospheric layers, where the scattering is mainly determined by the molecular component, are used for the lidar calibration. Sensing paths of emissions in industrial regions are close to horizontal. In this case, the data of path measurements of aerosol plume optical depth or local nephelometric measurements in the nearest lidar zone can be used for lidar calibration.

At present, more and more lidar stations are equipped with solar radiometers, thus becoming integrated stations of lidar and radiometric aerosol monitoring. Radiometric data can also be quite effective in lidar system calibration.⁶ In this case additional vertical lidar measurements are required. The value of A can be determined from the equation $A = S(l_\infty)/\beta_\infty T_\infty^2$, where " ∞ " means the value of corresponding parameter at the reference point at a height of about 10 km; β_∞ is the coefficient of backscattering, which is close to molecular; T_∞ is the atmospheric aerosol attenuation measured with a solar photometer.

A disadvantage of this technique for local calibration is a large fractional error of $S(l_\infty)$ measurements. Another way of calibration is calculation of integral (8) over some atmospheric layer by the equation

$$A = 2Q(\infty, 0) \left[1 - T_\infty^2 \exp\left(-2 \int_0^\infty \sigma_m \gamma_a / \gamma_m dl\right) \right]^{-1}. \quad (9)$$

The parameters T_∞ and γ_a can be determined from the scanning solar photometer measurements.

Contaminant concentration integrals over a segment of the sensing path η are calculated from the measured optical depths $\tau_a(l_2, l_1)$ using the empirical relationships from Ref. 1.

Possible experimental schemes

Consider two experimental schemes to assess the concentration integral over a plume cross section. In the first scheme, N pulses are sent along each sensing path. Then, in time T_1 required to change the path sensing angle, measurements along another path are

carried out. This procedure continues until the entire plume cross section is examined. In the second scheme, the sensing laser continuously and uniformly changes the path sensing angle, passing the angle range, where the plume is located, in two directions by turn.

In the first case, pulsing time can be presented as

$$t_{k,n} = (n-1)v^{-1} + (k-1)[(N-1)v^{-1} + T_1], \quad (10)$$

where n is the number of pulses, sent along the path k ; v is the pulsing frequency, Hz. Vertical coordinates of sensing beams in the plane of projection are determined by the equation

$$z_k = -0.5\Delta Z + \Delta Z(k-1)/(K-1), \quad (11)$$

where z_k is the vertical beam coordinate; K is the total number of paths; ΔZ is the range of vertical sensing coordinates near the plume (see Fig. 1).

In the second case, pulsing time can be presented by the equation

$$t_{k,m} = (k-1)v^{-1} + (m-1)[(K-1)v^{-1} + T_2], \quad (12)$$

and vertical coordinates in the plane of projection are determined as follows:

$$z_k = (-0.5\Delta Z + \Delta Z(k-1)/(K-1))(-1)^{m-1}. \quad (13)$$

In Eqs. (12) and (13), m is the number of passages of the flow cross section by the sensing beam; T_2 is the time required to change the scanning direction angle.

Let $\eta_{k,n}$ and $\eta_{k,m}$ be the integral concentrations, determined by the data of k -path lidar sensing with n th sensing pulse by the first scheme or in m th plume sensing by the second one. The concentration integral over the cross section (area integral concentration) is approximated by

$$I = \Delta Z \sum_{k=1}^K \sum_{n=1}^N \eta_{k,n} / N, \quad (14)$$

$$I = \Delta Z \sum_{k=1}^K \sum_{m=1}^M \eta_{k,m} / M \quad (15)$$

for the first and second sensing schemes, respectively; M is the total number of passages of the flow cross section by the sensing beam.

Error in estimate of the contaminant concentration integral over a turbulent flow cross section

The I difference from the average concentration integral over cross section is caused by concentration pulsations and finiteness of the number of sensing beams. The error due to finiteness of the number K

of sensing paths can be assessed, assuming that the numbers of averaging pulses N and passages M is large enough, therefore the measured $\sum_{n=1}^N \eta_{k,n}/N$ and

$$\sum_{m=1}^M \eta_{k,m}/M$$

are close to the turbulence-averaged

integral concentration along the k th path. As it is experimentally shown¹¹ and follows from the plume model,¹² the dependence of the averaged integral concentration on the transversal coordinate in plumes is close to the Gaussian function. In case of the Gaussian profile of the integral concentration, sums (14) and (15) over k approximate the integral over z with an error of the order of several percents even in case of 5–7 sensing paths. Hence, to calculate the integral over the cross section, a few paths are sufficient for sensing the region of the probable plume location.

The error

$$\epsilon = \sqrt{(\bar{I}^2/\bar{I}^2) - 1} \cdot 100\% \quad (16)$$

of I measurements due to atmospheric turbulence is determined, as is evident from Eqs. (14)–(16), by statistical moments of the first and second order of the integral contaminant concentration along the plume segment of a sensing path, as well as by times of pulsing and coordinates of the sensing beams.

To calculate the error, the equations were used, obtained in Ref. 12 for the average integral concentration and its covariation with and without (for comparison) accounting for in-plume concentration fluctuations, i.e., virtually by the Gifford model.¹³ All calculations were made with the following initial parameters: an average wind velocity of 4 m/s; mean-square longitudinal pulsation component of wind velocity of 0.4 m/s and the vertical one of 0.3 m/s; Lagrangian time of horizontal velocity correlation of 240 s and of vertical one of 90 s; Euler time of horizontal velocity correlation of 40 s and of vertical one of 20 s; vertical size of initial cross section of 1 m; $K = 9$; and the range of vertical beam coordinates ΔZ approximately two times larger than the plume's transverse size.

The error, calculated for a lidar with a low operating frequency of 0.1 Hz, is shown in Fig. 2. Though lasers with such pulse frequency are not used now in practice, this frequency is taken as a limiting case of low frequencies.

The first experimental scheme is considered. The time of sensing path change $T_1 = 10$ s. Measuring time at $N = 1$ and 4 is 80 and 350 s, respectively. The ϵ maximum is nearly the cross section with maximal concentration fluctuations. When increasing by four times the number of averaging pulses, the error decreases less than by half, because the correlation time of the integral concentration (Fig. 3) is comparable with or larger than the interval between pulses.

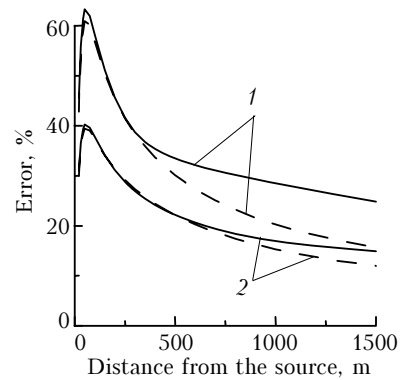


Fig. 2. The error of integral concentration sum (14) due to atmospheric turbulence as a function of distance from the emission source, calculated with (solid lines) and without (dashed lines) accounting for in-plume concentration fluctuations, following the first experimental scheme. The pulsing frequency is 0.1 Hz; time of sensing path change is 10 s; the number of pulses sent along the sensing path is 1 (1) and 4 (2).

The maximal error at $N = 4$ is about 40%, and it is less than 20% at distances from the source exceeding 500 m. The calculation results for the second experimental scheme are close to those in Fig. 2, i.e., both schemes are equally sensitive to the turbulence factor for low-frequency lasers.

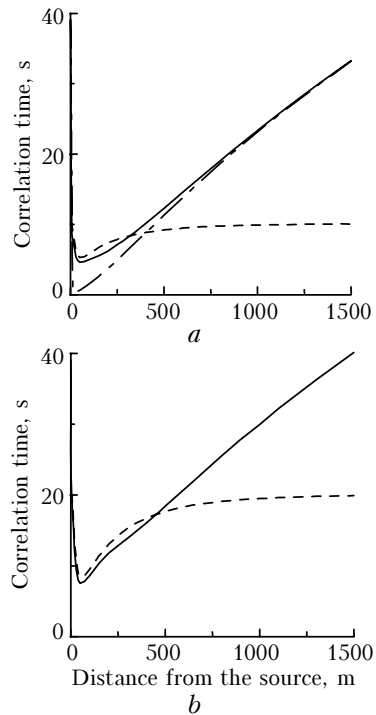


Fig. 3. Correlation time of integral concentration pulsations, determined by the e -fold drop, as a function of distance from initial cross section at the averaged plume axis at the distance $z = 0$ (a) and $z = \sqrt{L(x/U)}$ (b) from the axis, measured with (solid lines) and without (dashed ones) accounting for in-plume concentration fluctuations. The dashed-dotted line corresponds to the correlation time of area integral concentration pulsations, calculated with accounting for in-plume concentration fluctuations.

The calculated error ε for a lidar with operating frequency of 10 Hz is shown in Fig. 4. The second experimental scheme is considered. The time of sensing direction change $T_2 = 10$ s. Calculating times at $M = 1$ and 4 are 0.8 and 33 s, respectively.

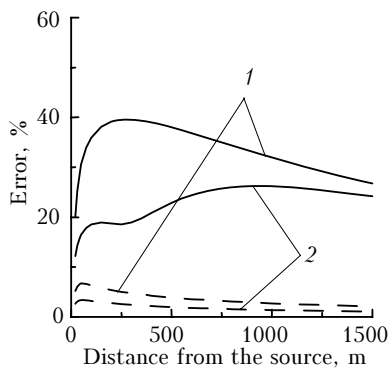


Fig. 4. The error of integral concentration sum (15) due to atmospheric turbulence as a function of distance from the emission source, calculated with (solid lines) and without (dashed lines) accounting for in-plume concentration fluctuations, following the second experimental scheme. Pulsing frequency is 10 Hz; time of sensing path change is 10 s; the number of pulses fed along the sensing path is 1 (1) and 4 (2).

In case of accounting for in-plume fluctuation, the maximum error at $M = 4$ is about 25%, and it is less than 20% at the distances from the source exceeding 300 m. For a lidar with 10 Hz operating frequency and the sensing following the first experimental scheme, the calculation results at $N = 1$ and 4 are closely equal to one another and the data for $M = 1$ in Fig. 4. The absence of averaging effect in this case is explained by very high pulsing frequency and, correspondingly, short averaging time in comparison with the correlation time of the linear integral concentration.

An advantage of the second experimental scheme in case of a high-frequency laser is a shorter averaging time, required for obtaining comparable accuracy levels. The minimal length of experiment, required for the R -fold decrease of the error in comparison with the case of $M = 1$, approximately equals to the correlation time of area integral concentration (integral over cross section) multiplied by R^2 . Since the correlation time of the integral over cross section approximately equals to the correlation time of the concentration integral over the sight line, than the same error decrease in the first experimental scheme takes place at only one space point. If to take into account the comparability of the initial measurement errors without averaging (at $N = M = 1$) in both schemes, it can be concluded that the measuring time in the first case is K times longer than in the second one.

Besides, the scheme with a high-frequency laser, capable to scan the plume's cross section much faster than the integral concentration correlation time, approximates to the scheme of a slit socket,

completely covering the vertical plume's cross section by the laser beam for one pulsing without scanning. In this case, fluctuations of I are totally defined by only the in-plume concentration fluctuations, since the I fluctuations due to displacement of the plume as a whole are suppressed. That is why the results in Fig. 4 calculated with and without accounting for in-plume concentration fluctuations differ essentially.

To decrease the error caused by plume instability, it is necessary to increase the number of sensing pulses and the measuring time. However, mesoscale wind velocity fluctuations in the atmosphere, characterized by times from several minutes to several hours and resulting in variations of average wind velocity U , are needed to be taken into account. The extreme measurement accuracy of the emission source capacity is limited by the wind velocity variability. According to Ref. 14, the typical relative wind velocity variability at a height of 121 m for 5, 10, 30, and 60 min is 17, 19, 24, and 29%, respectively.

Hence, the calculation error of the integral of concentration over plume cross section decreases with an increase of the averaging time, while the uncertainty of average wind velocity increases. Therefore, such measurement duration is optimal, at which the above error closely equals to the uncertainty of average wind velocity. As it follows from the above study, the best accuracy in calculating the emission source capacity under these conditions can be gained with the use of a high-frequency laser and the second experimental scheme.

Conclusion

Thus, both experimental schemes turn out to be equivalent when using a low-frequency laser with the frequency lower than or comparable with the inverse correlation time of the linear integral concentration. For a high-frequency laser, capable to scan the plume cross section much faster than the correlation time of linear integral concentration, the measurement error in the second experimental scheme decreases as compared with the first one due to suppression of fluctuations, caused by the displacement of the plume as a whole. Another advantage of the second scheme over the first one in case of a high-frequency laser is a shorter averaging time, required to obtain the comparable levels of accuracy, which is important under conditions of unstable atmosphere.

Acknowledgements

This work was financially supported in part by the Belorussian Republican Foundation for Basic Research (Project F05BR-008).

References

1. V.E. Zuev, B.V. Kaul, I.V. Samokhvalov, K.I. Kirkov, and V.I. Tsanev, *Laser Sensing of Industrial Aerosols* (Nauka, Novosibirsk, 1986), 188 pp.

2. Yu.S. Balin and I.A. Rasenkov, *Atmos. Oceanic Opt.* **6**, No. 2, 104–114 (1993).
3. A.P. Ivanov, A.P. Chaykovskii, F.P. Osipenko, I.S. Khutko, M.M. Korol', V.N. Shcherbakov, V.P. Kabashnikov, A.I. Bril', B.M. Popov, A.A. Kovalev, A.M. Samusenko, and M.A. Drugachenok, *Atmos. Oceanic Opt.* **11**, No. 4, 322–330 (1998).
4. M. Beniston, J.P. Wolf, M. Beniston-Rebetez, H.J. Kolsch, P. Rairoux, and L. Woste, *J. Geophys. Res.* D **95**, No. 7, 9879–9894 (1990).
5. L. Choulepnikoff, H. Van den Bergh, B. Calpini, and V. Mitev, in: *Encyclopedia of Environmental Analysis and Remediation*, R.A. Meyers, ed., (John Wiley&Sons, Inc., 1998), pp. 4873–4909.
6. A. Chaikovsky, A. Ivanov, M. Korol, A. Slesar, S. Denisov, F. Osipenko, I. Hutko, O. Dubovik, B. Holben, and Ph. Goloub, *Proc. SPIE* **6160**, 117–125 (2005).
7. V.A. Banakh and I.N. Smalikho, *Atmos. Oceanic Opt.* **4**, No. 10, 732–735 (1991).
8. V.A. Banakh, V.L. Mironov, I.N. Morskii, I.N. Smalikho, and I.A. Sutorikhin, *Atmos. Oceanic Opt.* **6**, No. 10, 739–743 (1993).
9. E.V. Bruyatskii, *Turbulent Stratified Jet Streams* (Naukova Dumka, Kiev, 1986), 295 pp.
10. F.T. Hieastadt and H. Van Dope, eds., *Atmospheric Turbulence and Pollution Propagation Simulation* [Russian translation] (Gidrometeoizdat, Leningrad, 1985), 351 pp.
11. N.L. Byzova, E.K. Garger, and V.N. Ivanov, *Experimental Study of Atmospheric Diffusion and Calculations of Contaminant Dispersion* (Gidrometeoizdat, Leningrad, 1991), 297 pp.
12. V.P. Kabashnikov and A.P. Chaykovskii, *Atmos. Oceanic Opt.* **20**, No. 1, 65–71 (2007).
13. F.A. Gifford, in: *Atmospheric Diffusion and Air Pollution* (Foreign Literature Press, Moscow, 1962), pp. 143–186.
14. *Atmosphere*, Handbook (Gidrometeoizdat, Leningrad, 1991), 509 pp.